

L. Mendoza<sup>1,2</sup>, C. Bianchi<sup>1,2</sup>, L. Fernández<sup>1,2</sup>, M. P. Natali<sup>1,2</sup>, A. Meza<sup>1,2</sup> and J. Moirano<sup>1</sup>,

<sup>1</sup> Laboratorio MAGGIA, Facultad de Ciencias Astronómicas y Geofísicas (FCAG), Universidad Nacional de La Plata (UNLP), La Plata, Argentina

<sup>2</sup> Consejo Nacional de Investigaciones Científicas y Técnicas (CONICET), Argentina

## 1 Introduction

Although the past decade has seen a significant development of the GNSS infrastructure in Central and South America, its potential for atmospheric water vapour monitoring has not been fully exploited. With this in mind, we have performed a regional, seven-year long and homogeneous analysis, comprising 136 GNSS tracking stations, obtaining high-rate and continuous observations of column integrated water vapour (IWV) and troposphere zenith total delay (ZTD).

As a preliminary application we have computed regional and local trends of water vapour content, together with realistic uncertainties, studying the correlation between these parameters and several climate regimes. In addition, we have analysed the regional performance of the troposphere model GPT2w (Böhm et al., 2015).

## 2 Methods

### GNSS data analysis

The observations were processed with the *Bernese GNSS Software* (Dach et al., 2015), at a double-difference level, and models recommended by the International Earth Rotation and Reference Systems Service (IERS) were used (Petit and Luzum, 2010).

In addition, troposphere zenith total delays (ZTDs) were modelled as 30-minutes linear piecewise estimates, applying the wet term of the Vienna Mapping Function 1 (VMF1, Böhm et al., 2006b), together with daily gradients according to Chen and Herring (1997).

A homogeneous set of reprocessed GPS+GLONASS precise orbits and clocks, computed by the Center for Orbit Determination in Europe (CODE) were used. In particular, we made use of the *co2* orbits, clocks and EOPs generated, as part of CODE's repro2 re-analysis, from three-day long-arc solutions (Steigenberger et al., 2014).

### Computation of IWV time series

Zenith hydrostatic delays (ZHDs) were computed according to Davis et al. (1985), employing observed atmospheric pressures. Then, the computed ZHDs were subtracted from the observed ZTDs to retrieve the wet terms (i.e., ZWDs). Finally, the ZWDs were scaled by a proportionality constant, as described by Askne and Nordius (1987), to obtain IWV estimates every 30 minutes.

We employed atmospheric pressure data sets provided by the University of Wyoming (UW), by the National Oceanic and Atmospheric Administration (NOAA) and by the IGS (RINEX m-files).

We derived the weighted mean temperature ( $T_m$ ) from the 6-hourly model levels of the ERA-Interim NWM (Dee et al., 2011). For each GNSS site,  $T_m$  was computed at the nearest four grid nodes of the NWM, integrating from the upper model level down to the geopotential height of the GNSS benchmark, and then interpolating linearly at the site's location and at the observation epoch.



Figure 1: IGS operational products with respect to this work.

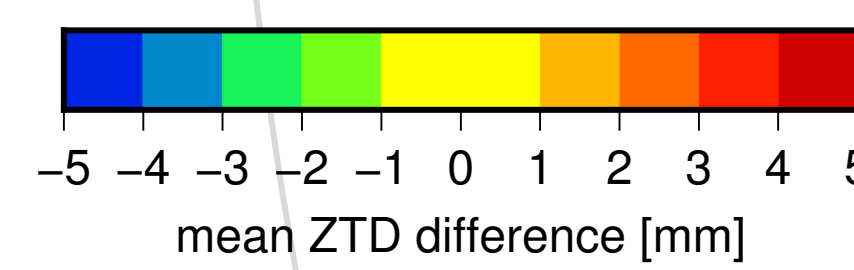
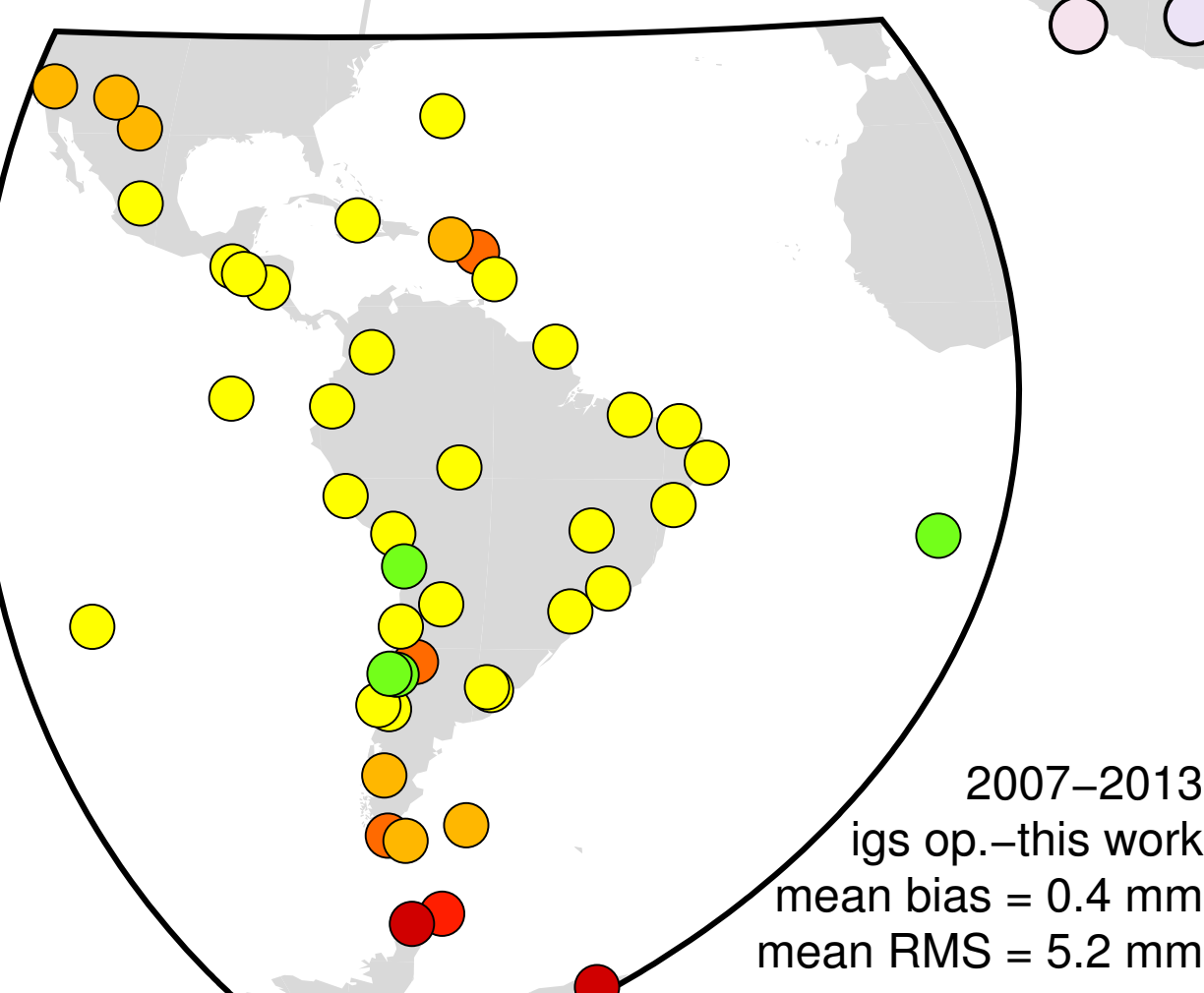
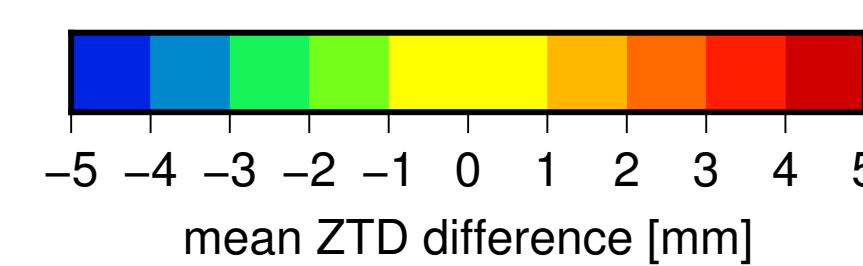
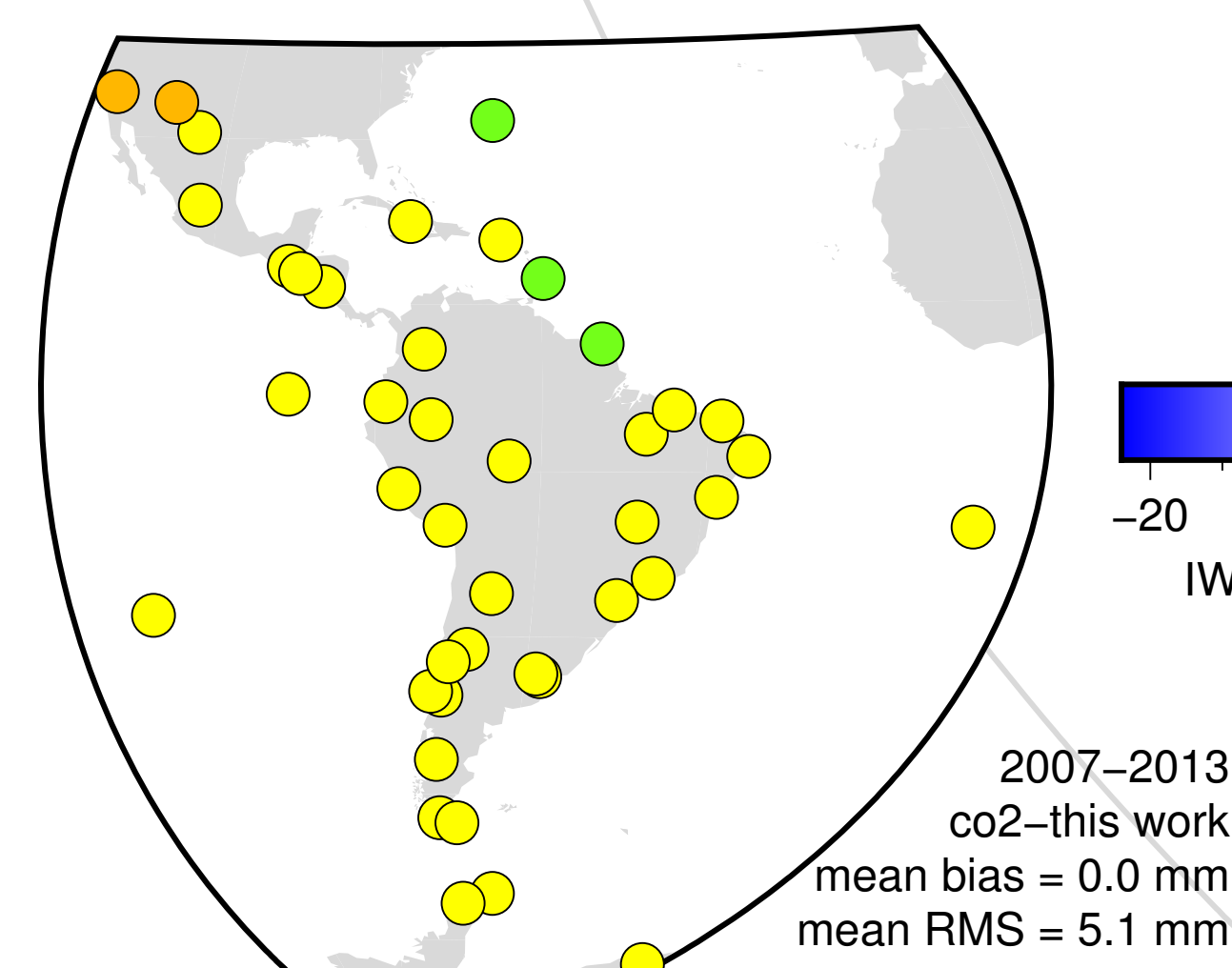


Figure 2: repro2 co2 solutions (CODE) with respect to this work.



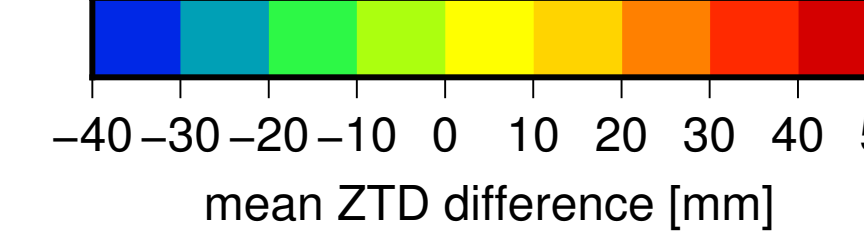
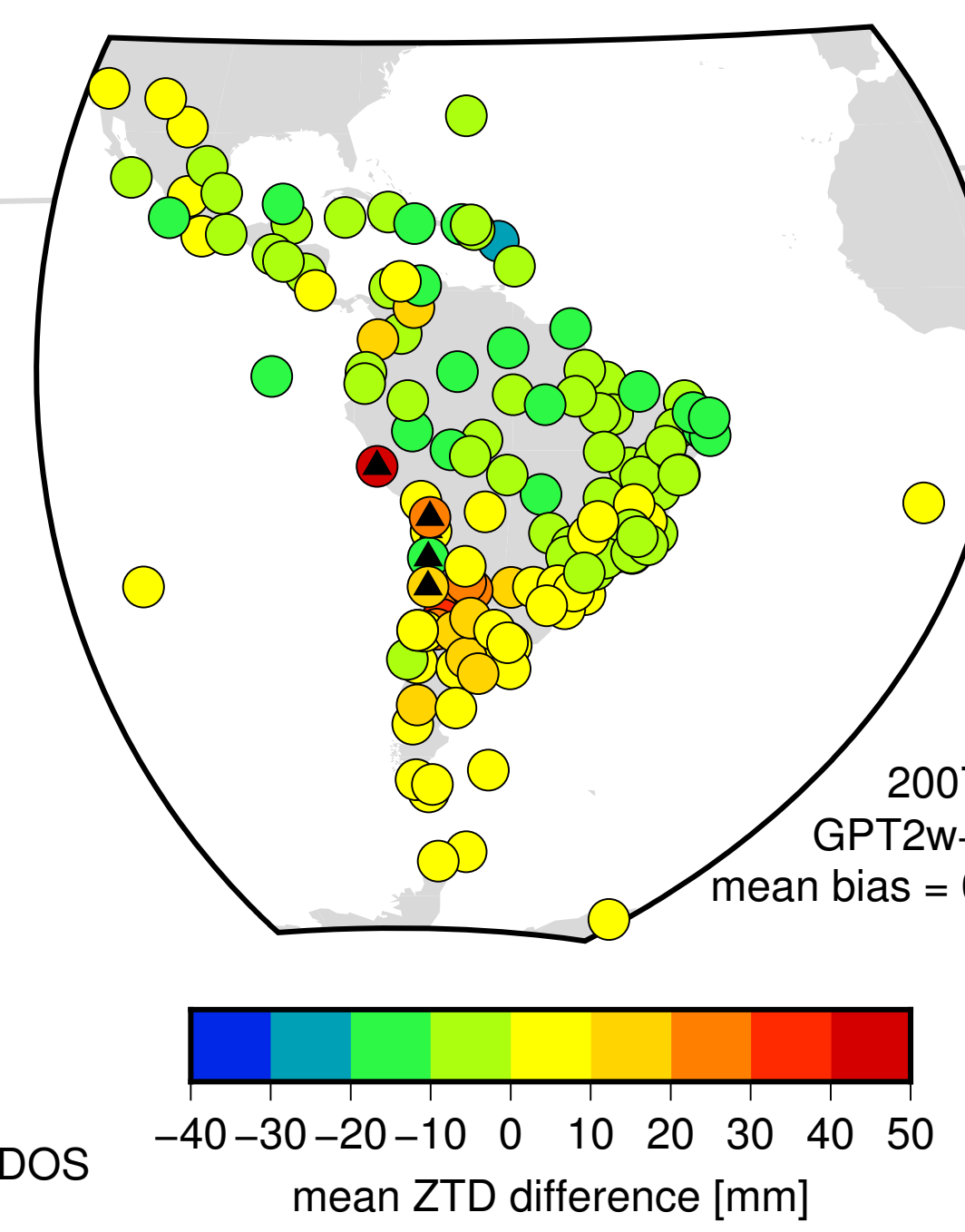
## References

Askne, J. and Nordius, H. (1987). Estimation of tropospheric delay for microwaves from surface weather data. *Radio Sci.*, 22(3):379–386.

Böhm, J., Möller, G., Schindelegger, M., Pain, G., and Weber, R. (2015). Development of an improved empirical model for slant delays in the troposphere (gpt2w). *GPS Solut.*, 19(3):433–441.

Böhm, J., Niell, A., Tregoning, P., and Schuh, H. (2006a). Global Mapping Function (GMF): A new empirical mapping function based on numerical weather model data. *Geophys. Res. Lett.*, 33(7).

Figure 3: regional assessment of the GPT2w blind model: mean differences between modelled (GPT2w) and observed (GNSS) ZTDs. The black triangles indicate those sites where the orthometric height difference, between the nearest GPT2w topographic grid nodes and the corresponding GNSS benchmark, exceeds 2500 m.



Climate Type	Mean IWV Trend in % per decade	Number of Sites
Tropical (NH and SH)	+0.7 ± 1.1	35 <sup>†</sup>
Temperate (SH)	-1.8 ± 1.4	20
Arid (NH)	-6.0 ± 4.6	5
Arid (SH)	+6.0 ± 5.2	4

<sup>†</sup>The site ISPA was not included (Easter Island).

Table 3: Mean IWV trends computed within regions of similar climate types, in Central and South America and the Caribbean, between January 2007 and December 2013. NH and SH means Northern and Southern Hemisphere, respectively.

Site	Mean Diff. <sup>1</sup> kg m <sup>-2</sup>	Std. Dev. kg m <sup>-2</sup>	Number Of Samples <sup>2</sup>
BDOS	0.29	2.75	1077
BELE	-0.18	1.82	1395
BOAV	-0.10	1.98	1532
BOGT	0.00	1.01	1594
CUIB	0.04	1.98	1716
IGM1	-0.43	1.55	1436
MSCG	0.04	1.55	1071
MZAC	0.68	1.28	700
PARC	0.41	1.25	1236
PEPE	-0.59	1.83	1592
POAL	-0.43	2.11	1325
POLI	-0.50	1.51	1798
POVE	0.19	2.03	1698

<sup>1</sup>Radioonde minus GNSS. <sup>2</sup>Daily samples at 12:00 UTC.

Table 2: Comparison between IWV measured with co-located radiosondes and our GNSS derived estimates.

Figure 6: Observed local IWV trends.

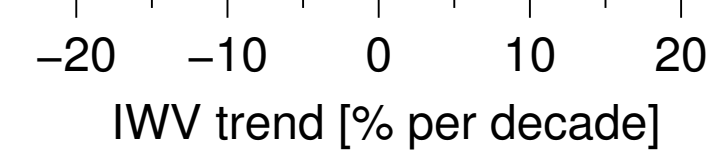


Figure 4: Mean IWV estimates.

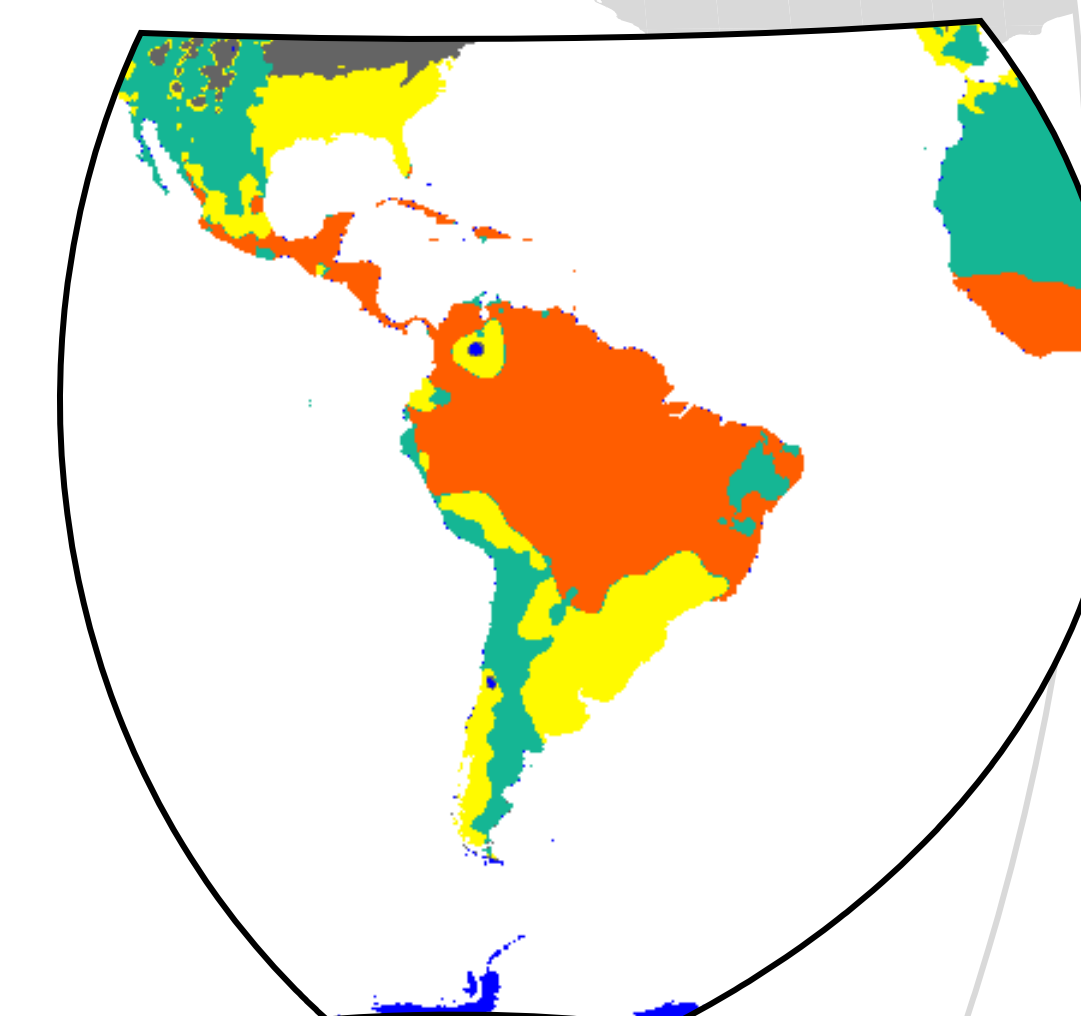
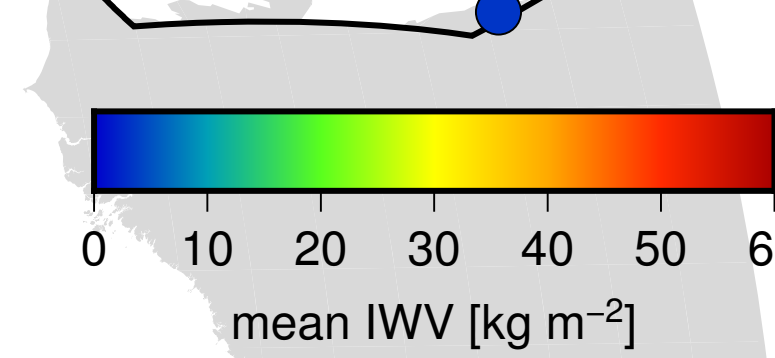
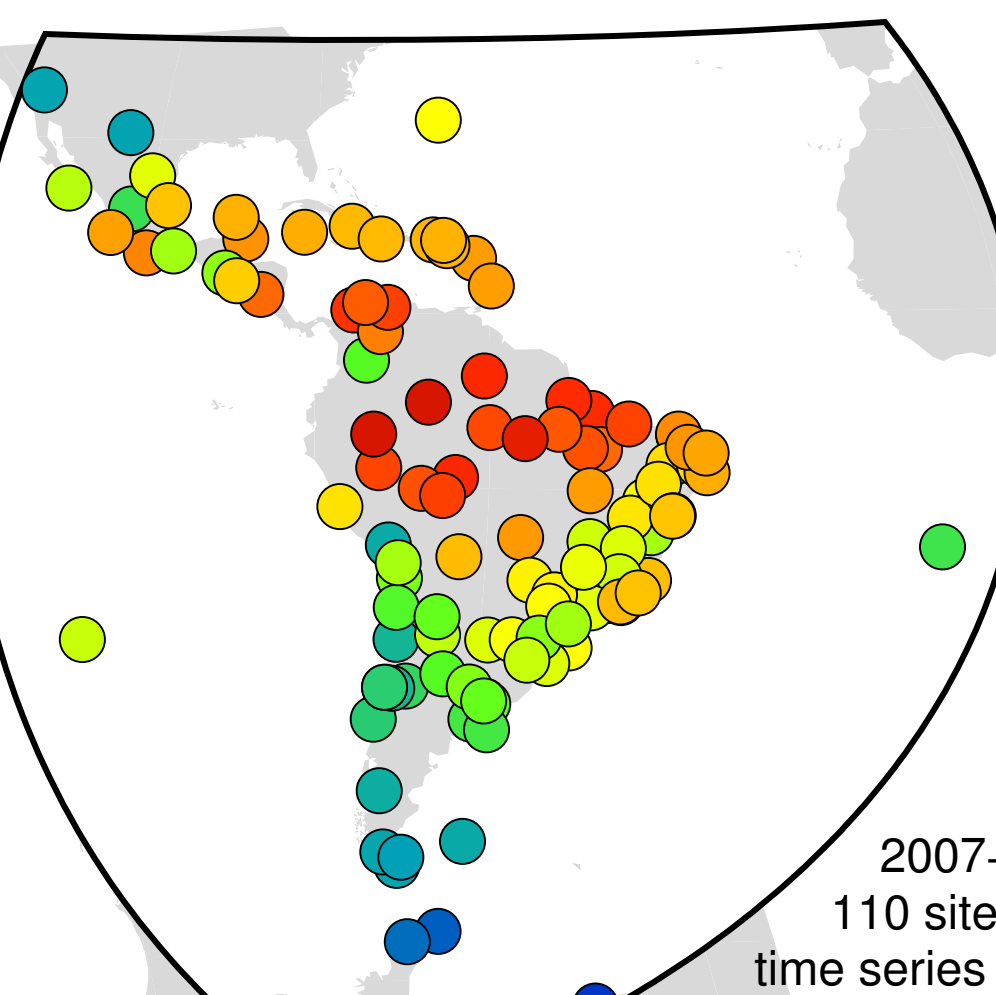


Figure 5: Köppen-Geiger (broad) climate types for the Americas according to Peel et al. (2007).

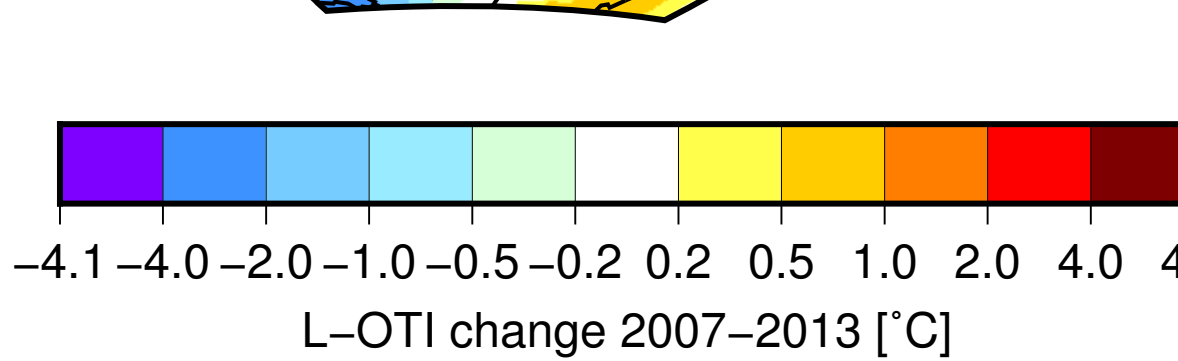
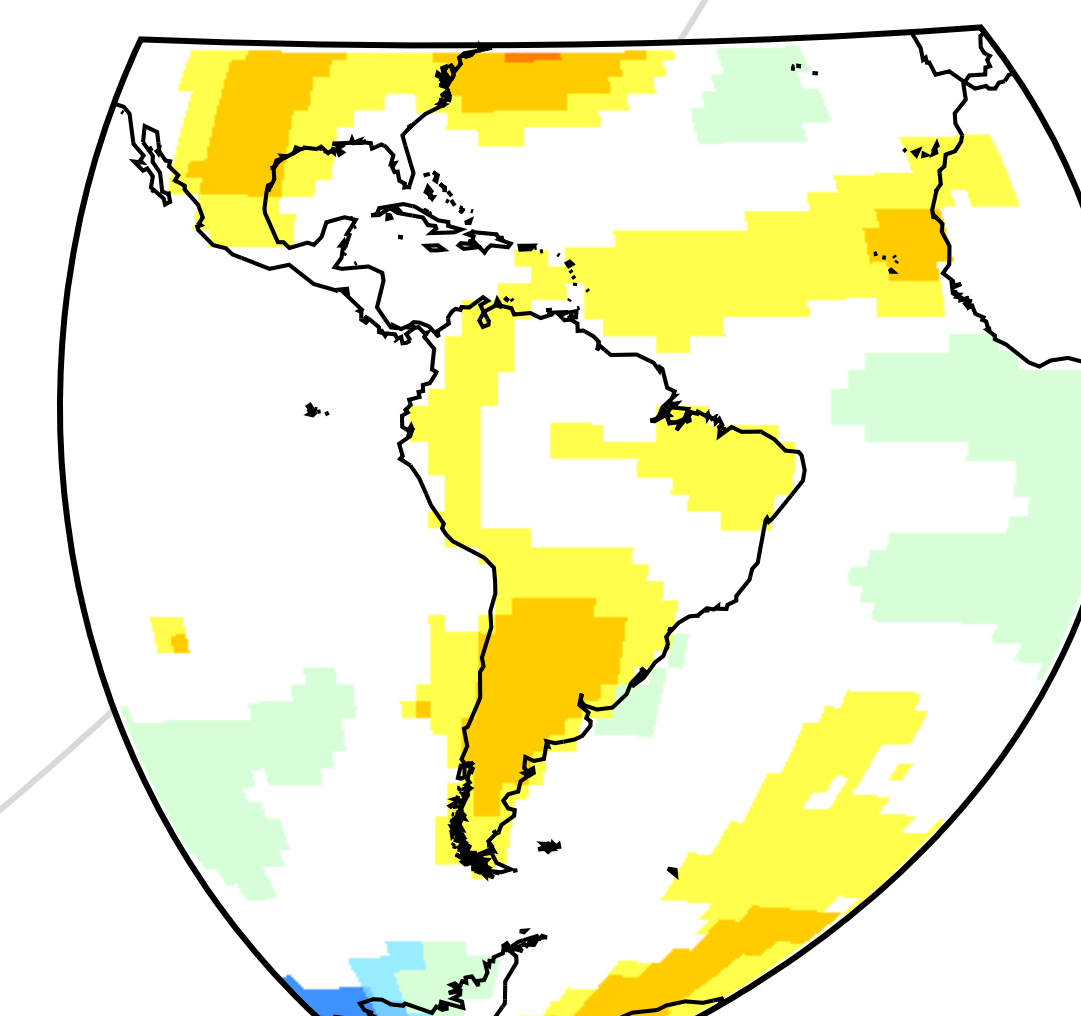


Figure 7: Land-Ocean Temperature Index (L-OTI) change, during 2007–2013, according to GISTEMP Team (2016) (see also Hansen et al., 2010).

## 3 Results

### GNSS processing evaluation

We performed a site-per-site comparison with three different data sets produced by IGS ACs (Table 1). In general, all the compared ZTD solutions show a good agreement, with long-term mean

inter-biases lower than half a millimetre. The quality of our ZTD estimates is on par with both IGS reprocessing analysis and it surpasses the consistency of the operational products (Figs. 1 and 2).

Solution	Analysis Center	Mapping Function	Elevation Cutoff Angle [deg]	Sampling Rate [s]	Remarks	Sites in Common With This Work
operational	JPL	NIELL (Niell, 1996)	7	300	until 16 April 2011	45
operational	USNO	WET GMF (Böhm et al., 2006a)	7	300	since 17 April 2011	45
repro2 co2	CODE	WET VMF (Böhm et al., 2006b)	3	7200		42
repro2 jp2	JPL	GPT2 (Lagler et al., 2013)	7	300	no gradients	44

Table 1: The IGS products employed for the ZTD estimates evaluation.

### Troposphere model assessment

The performance of the GPT2w model, in Central and South America, results within the ranges reported by Böhm et al. (2015).

probably inherited from the underlying NWM, in this case ERA-Interim (Dee et al., 2011).

However, the modelled ZTDs seems to be systematically underestimated, up to 20 mm, at sites in wet regions, while modelled values at arid and temperate regions result, on average, overestimated up to 20 mm (Fig. 3). These biases are

Some of the systematic biases observed in South America seems to be related to the insufficient resolution of the GPT2w's underlying topographic model to accurately reproduce the highly variable topography near the Andes.

### IWV retrieving and analysis

Our IWV estimates (Fig. 4) were compared with co-located radiosondes observations, provided also by UW. The accuracy of the IWV estimates is always better than 3 kg m<sup>-2</sup>, and satisfies the requirement for regional climate studies within the Global Climate Observing System (GCOS) specifications.

tropical areas in Central and South America and the Caribbean, as a whole, seem to be slowly moistening

The observed moistening of the troposphere, in some arid regions in South America, also coincides with a moderate increase in surface temperatures (Fig. 7).

The estimated trends do correlate within regions with similar climate type (Table 3, Fig. 5). In particular, temperate regions in South America seem to be drying (Fig. 6), whereas the

It is worth noting that the estimated IWV trends are only valid for the given time span and should not be regarded as long-term signals without further considerations.

## 4 Conclusions

Evidence of drying of the troposphere over temperate regions in South America has been found, at a mean IWV rate of approximately 2% per decade, particularly in southern Brazil and central-eastern Argentina.

This regional, multi-year, GNSS analysis has made also possible a robust performance assessment of the GPT2w blind model.

The results also suggests a slow troposphere moistening at the tropics, but this inference is less conclusive.

The results showed the good general agreement between observed and modelled mean delays, but also revealed some limitations (up to 20 mm in ZTD).

## Acknowledgements

We would like to thank the people, organisations and agencies responsible to collect, compute, maintain and openly provide the observations and the products employed in this work: International GNSS Service (IGS) and its associated Analysis Centers, Système d'Observation du Niveau des Eaux Littorales (SONEL) and its many contributing organisations, Instituto Brasileiro de Geografia e Estatística (IBGE, Brasil), Instituto Geográfico Nacional (IGN, Argentina), University of Wyoming (UW, USA), National Oceanic and Atmospheric Administration (NOAA, USA) and Servicio Meteorológico Nacional (SMN, Argentina). Also, we thank the people at PANGAEA (<http://www.pangaea.de>).

Peubey, C., de Rosnay, P., Tavaloto, C., Thépaut, J.-N., and Vitar, F. (2011). The era-interim reanalysis: configuration and performance of the data assimilation system. *Quart. J. Roy. Meteor. Soc.*, 137(656):553–597.

GISTEMP Team (2016). Giss surface temperature analysis (gistemp), nasa goddard institute for space studies. Dataset accessed 2016-05-30.

Hansen, J., Ruedy, R., Sato, M., and Lo, K. (2010). Global surface temperature change. *Rev. Geophys.*, 48(4).

Lagler, K., Schindelegger, M., Böhm, J., Krásná, H., and Nilsson, T. (2013). Gpt2: Empirical slant delay model for radio space geodetic techniques. *Geophys. Res. Lett.*, 40(6):1069–1073.

Steinbach, A., and Thaller, D. (2015). *Bernese GNSS Software Version 5.2*. University of Bern.

Davis, J. L., Herring, T. A., Shapiro, I. I., Rogers, A. E. E., and Elgered, G. (1985). Geodesy by radio interferometry: Effects of atmospheric modeling errors on estimates of baseline length. *Radio Sci.*, 20(6):1593–1607.

Dee, D. P., Uppala, S. M., Simmons, A. J., Berrisford, P., Poli, P., Kobayashi, S., Andrae, U., Balmaseda, M. A., Balsamo, G., Bauer, P., Bechtold, P., Bejari, A. C. M., van de Berg, L., Bidlot, J., Bormann, N., Delsol, C., Dragani, R., Fuentes, M., Geer, A. J., Haimberger, L., Healy, S. B., Hersbach, H., Hölm, E. V., Isaksen, I., Kållberg, P., Köhler, M., Matricardi, M., McNally, A. P., Monge-Sanz, B. M., Morcrette, J.-J., Park, B.-K.,

Böhm, J., Werl, B., and Schuh, H. (2006b). Troposphere mapping functions for gps and very long baseline interferometry from european centre for medium-range weather forecasts operational analysis data. *J. Geophys. Res. Solid Earth*, 111(B2).

Chen, G. and Herring, T. A. (1997). Effects of atmospheric azimuthal asymmetry on the analysis of space geodetic data. *J. Geophys. Res. Solid Earth*, 102(B9):20489–20502.

Dach, R., Andritsch, F., Arnold, D., Bertone, S., Fridez, P., Jäggi, A., Jean, Y., Maier, A., Mervart, L., Meyer, U., Orliac, E., Ortiz-Gea, E., Prange, L., Scaramuzza, S., Schaer, S., Sidorov, D., Sušnik, A., Villiger, A., Walsler, P., Baumann, C., Beutler, G., Bock, H., Gäde, A., Lutz, S., Meindl, M., Ostini, L., Sośnica, K.,

Steigenberger, P., Hugentobler, U., Lutz, S., and Dach, R. (2014). Code contribution to the 2nd igs reprocessing. In *IGS Workshop 2014*. Astronomisches Institut der Universität Bern, Bern, Switzerland and Technische Universität, München, München, Germany.

Niell, A. (1996). Global Mapping Function for the Atmosphere Delay at radio Wavelength. *J. Geophys. Res.*, 101(B2):3227–3246.

Peel, M. C., Finlayson, B. L., and McMahon, T. A. (2007). Updated world map of the Köppen-Geiger climate classification. *Hydro. Earth Syst. Sci.*, 11(5):1633–1644.

Petit, G. and Luzum, B. (2010). IERS Conventions (2010). Technical Report 36, IERS Conventions Centre.